HHS Public Access

Author manuscript

J Immunol. Author manuscript; available in PMC 2019 November 01.

Published in final edited form as:

J Immunol. 2018 November 01; 201(9): 2744–2752. doi:10.4049/jimmunol.1800885.

Combined HDAC and BET inhibition enhances melanoma vaccine immunogenicity and efficacy

Alexander Badamchi-Zadeh[*], **Kelly D. Moynihan**[†], **Rafael A. Larocca**[*], **Malika Aid**[*], **Nicholas M. Provine**[*], **M. Justin Iampietro**[*], **Ekaterina Kinnear**[‡], **Pablo Penaloza-MacMaster**[§], **Peter Abbink**[*], **Eryn Blass**[*], **John S. Tregoning**[‡], **Darrell J. Irvine**[†,¶,‖], and **Dan H. Barouch**[#,*,¶]

* Center for Virology and Vaccine Research, Beth Israel Deaconess Medical Center, Harvard Medical School, Boston, MA 02215, USA.

† Koch Institute for Integrative Cancer Research, Massachusetts Institute of Technology (MIT), Cambridge, MA, USA.

‡ Department of Medicine, Imperial College London, St. Mary's Campus, London, UK.

§ Department of Microbiology-Immunology, Feinberg School of Medicine, Northwestern University, Chicago, IL 60611, USA.

¶ Ragon Institute of Massachusetts General Hospital, Massachusetts Institute of Technology and Harvard University, Cambridge, MA 02139, USA.

‖ Howard Hughes Medical Institute, Chevy Chase, MD 20815, USA.

Abstract

The combined inhibition of histone deacetylases (HDAC) and the proteins of the bromo and extra terminal (BET) family have recently shown therapeutic efficacy against melanoma, pancreatic ductal adenocarcinoma, testicular and lymphoma cancers in murine studies. However, in such studies the role of the immune system in therapeutically controlling these cancers has not been explored. We sought to investigate the effect of the HDAC inhibitor romidepsi n (RMD) and the BET inhibitor IBET151, both singly and in combination, on vaccine elicited immune responses. C57BL/6 mice were immunized with differing vaccine systems (adenoviral, protein) in prime-boost regimens, under treatment with RMD, IBET151, or RMD+IBET151. The combined administration of RMD+IBET151 during vaccination resulted in a significant increase in the frequency and number of antigen-specific CD8 T cells. RMD+IBET151 treatment significantly increased the frequency of vaccine-elicited IFN-γ+ splenic CD8 T cells and conferred superior therapeutic and prophylactic protection against B16-OVA melanoma. RNA-Seq analyses revealed strong transcriptional similarity between RMD+IBET151 and untreated antigen-specific CD8 T cells, except in apoptosis and IL-6 signaling-related genes that were differentially expressed. Serum IL-6 was significantly increased *in vivo* following RMD+IBET151 treatment, with recombinant IL-6 administration replicating the effect of RMD+IBET151 treatment on vaccine-elicited CD8 T cell responses. IL-6 sufficiency for protection was not assessed. Combined HDAC and BET inhibition resulted in greater vaccine-elicited CD8 T cell responses and enhanced

Corresponding author: Phone: 617-735-4485; Fax: 617-735-4566; dbarouch@bidmc.harvard.edu.

The authors have no financial conflicts of interest.

therapeutic and prophylactic protection against B16-OVA melanoma. Increased IL-6 production and the differential expression of pro- and anti-apoptotic genes following RMD+IBET151 treatment are likely contributors to the enhanced cancer vaccine responses.

Introduction

The combined inhibition of two classes of epigenetic regulators, histone deacetylases (HDACs) and bromodomain and extra-terminal proteins (BET), has recently shown therapeutic efficacy against multiple cancer types including pancreatic ductal adenocarcinoma, testicular, lymphoma, and melanoma (1–4). Proposed mechanisms for the enhanced tumor killing by the combination of HDAC and BET inhibition includes the suppression of AKT and YAP signaling (3), the induction of apoptosis over cell-cycle arrest in Myc-induced cells (2), the transcriptional induction of p57 (1), and anti-angiogenesis (4). In addition to intrinsic tumor cell apoptosis, it is now established that CD8 T cells of the mammalian immune system can recognize and kill tumor cells (5). This has resulted in a paradigm shift in cancer therapy, whereby immunotherapies exploiting this T cell ability have resulted in better clinical outcomes than some conventional cancer therapies (6). CD8 T cell differentiation and functionality is tightly regulated under epigenetic controls (7–9), suggesting potential immunotherapeutic involvement in the HDAC and BET inhibitor cancer therapy.

In this study, we use the ability of vaccines to induce antigen-specific T cell responses to assess changes to T cell differentiation and function following HDAC and BET inhibition. We report that the combination of these two inhibitors significantly increase vaccine-elicited CD8 T cell number, and confer enhanced prophylactic and therapeutic protection against melanoma when used with vaccination. HDAC and BET inhibition increase elicited CD8 T cells through transcriptionally altering their apoptosis and IL-6/JAK/STAT related genes following cancer vaccination.

Materials and Methods

Mice, immunizations, and Listeria challenge.

Female 6–10 week old C57BL/6 mice (The Jackson Laboratory, Bar Harbor, ME) were kept in accordance with the Institutional Animal Care and Use Committee guidelines of Beth Israel Deaconess Medical Center. Mice received immunizations of E1/E3 deleted Ad serotype 26 (Ad26) and Ad serotype 5 (Ad5) expressing either SIVmac239 Gag (Gag), SIVmac239 Env (Env), ovalbumin (OVA), or the ovalbumin immunodominant epitope SIINFEKL, as described previously (10, 11). Vectors were administered at 10^9 or 10^7 viral particles (vp) intramuscularly in the quadricep in 50 μl volume. Ovalbumin (Low Endo, Worthington Biochemical Corporation) and CpG (ODN 1826, Invivogen) or CDN (c-di-AMP VacciGrade, Invivogen) were administered at 10 μg and 10 μg respectively in 100 μl subcutaneously at the tail base. Mice were challenged with either 1×10^5 or 5×10^5 CFU of recombinant *Listeria monocytogenes* expressing the OVA epitope SIINFEKL (Lm-OVA) by i.v. injection. *L. monocytogenes* bacterial load was calculated by plated splenocytes on BHI-Agar plates, as described previously (12).

Epigenetic inhibitors.

Romidepsin (RMD; Selleckchem) was suspended in sterile PBS plus 0.5% DMSO and injected i.p. at 1 mg/kg dose (13, 14) with a single dose at time of vaccination. IBET151 (GSK1210151A; Selleckchem) was suspended in sterile PBS plus 30% DMSO and injected i.p. at 30 mg/kg (15), with a single dose at time of vaccination. Combined administration of RMD and IBET151 was performed i.p. at the same dosages above, in a final volume of 250 μl, at a single dose at time of vaccination. Vehicle control mice received 250 μl of sterile PBS plus 30% DMSO i.p.

mAb and cytokine administration.

The monoclonal anti-CD8a (clone 53–6.72; BioXCell) was administered i.p. at 500 μg every 7 days from d-1 prior to tumor injection to maintain CD8 T cell depletion. Anti-PD-ligand 1 (PD-L1; clone 10F.9G2; BioXCell), or isotype IgG2b (clone LTF-2; BioXCell) were administered by 200 μg i.p. injections, as described previously (16, 17) at d-1, d0, d1 and d3 with respect to vaccine boost. Mouse rIL-6 (R&D Systems) suspended in PBS was given at 60 ng i.p. daily from d0 to d3 at boost (18).

Luminex assay.

Serum samples were collected 6 h post vaccination and assayed using a Luminex bead-based multiplex ELISA (MILLIPLEX MAP Mouse Cytokine/Chemokine Magnetic Bead Panel, Millipore), according to manufacturer's instructions. Sample data was acquired on a Magpix instrument running Xponent software (Luminex Corp.) and analyzed using a 5-parameter logistic model.

Tumor cell culturing and inoculation.

B16-OVA cells were kindly provided by D. Irvine (MIT) and cultured in complete Dulbecco's modified Eagle's medium (DMEM, GE Healthcare Life Sciences), supplemented with 10% FBS and 200 μg/ml G418 (Invivogen). Cells were maintained at 37°C, 5% CO_2. An inoculum of 5×10^5 B16-OVA tumor cells was injected s.c. on the flank of mice in 50 μl sterile PBS. Tumor size was measured as area (longest dimension x perpendicular dimension), and mice euthanized when tumor area exceeded 100 mm^2.

Flow cytometry, intracellular cytokine staining, and cell sorting.

Lymphocytes were isolated from either the blood or spleen, stained, and analyzed by flow cytometry as previously described (19). Antibodies to CD8α (53–6.7), CD4 (RM4–5), CD44 (IM7), CD127 (A7R34), KLRG1 (2F1), PD-1 (RMPI-30), IFN-γ (XMG1.2), and Foxp3 (FJK-16S) were purchased from BD Biosciences, eBioscience, or BioLegend. Cell viability was assessed by LIVE/DEAD Fixable Aqua (Life Technologies). Antigen-specific cells were identified by MHC class I tetramer staining using either the AL11 peptide of Gag (AAVKNWMTQTL, H-2D^b) (20) or the immunodominant $OVA_{257–264}$ (SIINFEKL, H-2K^b) epitope from ovalbumin protein (21), with monomers provided by the NIH Tetramer Core Facility (Emory University, Atlanta, GA). For intraceullar cytokine staining, splenocytes were incubated for 5 h at 37°C with 1 μg/ml SIV_{mac239}Gag peptide pool. During peptide incubation, brefeldin A and monensin (BioLegend) were added. Cells were subsequently

washed, stained, and permeabilized with Cytofix/Cytoperm (BD Biosciences). Cells were acquired on an LSR II flow cytometer (BD Biosciences), or sorted on a FACSAria III Special Order (BD Biosciences) with >98% purity. Data were analyzed using FlowJo v.9.8.5 (Treestar).

RNA-Seq data acquisition and analysis.

Splenic CD8+ T cells were enriched by negative selection (CD8+ T cell isolation kit, Stemcell Technologies) prior to Db/SIINFEKL+CD44+CD8+ T cell sorting to >98% purity (data not shown). Sorted cells were stored at −80C in 1 ml of TRIzol. RNA extraction was performed using the RNeasy 96 QIAcube HT Kit (QIAGEN) per manufacturer's instructions. RNA concentration and quality was confirmed by Agilent's 2100 bioanalyzer (Agilent Technologies). A Low Input Total RNA library (Clontech SMARTer) was constructed, and sequenced on Illumina NS500 Pair-End 75bp at The Molecular Biology Core Facility at Dana-Farber Cancer Institute. Raw sequences in fastq format were aligned to the mouse reference genome (version mm10) using STAR (22) with default settings that include soft clipping using the following options: sjdbOverhang: 74; SortedByCoordinate: –quantMode; and TranscriptomeSAM: GeneCounts. Illumina adapters were cut using Trimmomatic (23). Only unique and concordant alignments were used for downstream analysis. Quantification and normalization of the mapped reads at the level of gene model were performed with edgeR (24). A p value cut-off of 0.05 was used to detect significant differential gene expression. Pathway analyses were performed using gene set enrichment analyses (GSEA) (25) with C2 gene sets. The enrichment of chromatin remodeling and IL-6/JAK/STAT3 pathways was assessed using the Fisher exact test and odds ratios calculated using the background population of all annotated mouse genes. All p values were adjusted for multiple testing using a cut-off of 0.05.

Quantitative immunoglobulin ELISA.

A quantitative immunoglobulin ELISA protocol described previously (26) was followed. Briefly, 0.5 μg/ml of either SIVmac239 Env or OVA protein coated ELISA plates were blocked with PBS/1% BSA/0.05% Tween-20. After washing, diluted serum samples were incubated with the plates for 1 h prior to further washing, and the addition of 1:4000 dilution of either anti-mouse IgG-, IgG1-, or IgG2a-HRP (Southern Biotech). The standard wells of anti-mouse Kappa (1:3200) and Lambda (1:3200) light chain (Serotec) coating were blocked and washed prior to adding purified IgG, IgG1 or IgG2a (Southern Biotech) starting at 1000 ng/ml. Samples and standards were developed with TMB and the reaction stopped after 5 min with Stop solution (KPL Inc.). Absorbance was read on a spectrophotometer at $OD_{450–500\ nm}$ with SoftMax Pro GxP v5 software.

Influenza Challenge.

6–8 week old female BALB/c mice were obtained from Harlan UK Ltd (Littlemore, Oxford, UK) and kept in specific-pathogen-free conditions in accordance with the United Kingdom's Home Office guidelines. All work was approved by the Animal Welfare and Ethical Review Board (AWERB) at Imperial College London. Mice were immunized intramuscularly with 0.005μg purified surface antigen from influenza strain H1N1 A/California/7/2009 (GSK Vaccines, Siena, Italy) twice with a minimum of 3 week interval between immunizations.

Mice received RMD+IBET151 intraperitoneally during boosting vaccination. For infections, H1N1 Influenza strain A/California/7/2009 was grown in Madin-Darby Canine Kidney (MDCK) cells, in serum free DMEM supplemented with 1μg/ml trypsin. Mice were anaesthetized using isoflurane and infected intranasally with 3×10^4 pfu influenza and weight loss was monitored daily.

Immune cells were assessed as described in Materials and Methods, but with the following antibodies: Influenza A H-2Kd HA533–541 pentamer R-PE (Proimmune, Oxford, UK), CD3-FITC (BD, Myrtle, UK), CD4- PE/Cy7 (BioLegend, CA, USA), CD8-APC-H7 (BD, Myrtle, UK). Analysis was performed on an LSRFortessa flow cytometer (BD) after collecting data on at least 50,000 Live CD3+ events.

Serum antibodies specific to Influenza HA1 were measured as described in above, with the exception that plates were coated with 1 μg/ml H1N1 surface protein, and absorbance was read at 450 nm on a FLUOstar spectrophotometer (BMG LABTECH GmbH, Ortenberg, Germany) and absorbance values for the standard titration were fitted with a four parameter logistic curve and unknown values were interpolated using BMG Omega software.

Statistical analysis.

Statistical analyses were performed using Prism 6.0 (GraphPad Software). Normality of the data was assessed using the Kolmogorov-Smirnov normality test, with non-parametric data analyzed by the Kruskal-Wallis test with Dunn's multiple comparison post-test (more than two groups) or the two-tailed Mann-Whitney U test (for two groups). For parametric data, a one-way ANOVA with Bonferroni's multiple comparison post-test (more than two groups) or an unpaired t-test (for two groups) was used. $P < 0.05$ was considered significant ($^{*}p < 0.05$, $^{**}p < 0.01$, $^{***}p < 0.001$).

Results

RMD+IBET151 treatment improves therapeutic adenoviral vaccination and reduces B16 melanoma burden.

To investigate the role of HDAC (RMD) and BET inhibition (IBET151) on cellular immune responses, the inhibitors were administered singly and in combination during Ad vector immunization. Mice were immunized with vectors expressing the HIV Gag gene in an Ad26 prime Ad5 boost regimen, which has been shown to generate robust, measurable, antigen-specific CD8 T cell responses (27). Mice were administered RMD, IBET151, RMD +IBET151 mixture, or PBS/DMSO vehicle control, by the i.p. route just prior to i.m. boost vaccination with Ad5.Gag. The combined administration of RMD+IBET151 resulted in a significant ($^{*}p < 0.05$) doubling of the frequency and number of Gag (epitope AL11) specific CD8 T cells circulating in the blood at day 7 after boost, compared to the inhibitors administered individually or the PBS/DMSO control (Fig. 1A). In addition, there was a significant increase in the frequency of CD8 T cells that produced IFN-γ upon ex-vivo restimulation in mice that were treated with the RMD+IBET151 combination compared to RMD or IBET151 alone ($^{**}p < 0.01$; Fig. 1B). RMD+IBET151 treatment did not significantly change the total number of circulating CD8 T cells (Fig. S1A), or the

percentage of regulatory Foxp3+ CD4 T cells (Fig. S1B). RMD+IBET151 treatment during priming and boosting vaccination provided the same antigen-specific CD8 T cell increase as RMD+IBET151 treatment at boosting alone (Fig. S1C). Therefore subsequent vaccinations only received RMD+IBET151 treatment at boost.

To evaluate the therapeutic efficacy of RMD+IBET151 treatment during vaccination against melanoma tumor progression, mice were primed with Ad26.OVA (10^7 vp), followed by the subcutaneous injection of 500,000 B16-OVA cells 28 days later. Eleven days after melanoma injection, mice were therapeutically treated with Ad5.SIINFEKL or Ad5.empty (10^9 vp), with or without RMD+IBET151 (Fig. 1C). RMD+IBET151 administration resulted in a significant increase in OVA specific SIINFEKL+ CD8 T cells at day 7 after Ad5.SIINFEKL treatment measured by tetramer staining ($^{*}p < 0.05$; Fig. S1D). The combined treatment of Ad5.SIINFEKL with RMD+IBET151 resulted in a significant regression in B16 melanoma tumor burden compared to Ad5.SIINFEKL treatment alone ($^{**}p < 0.01$; Fig. 1D) at day 4 after treatment. Although tumor load remained lower following Ad5.SIINFEKL + RMD +IBET151 therapy, this statistical significance was lost by day 7, and all treated mice succumbed to tumor growth and death (Fig. S1H). With a greater Ad26.OVA priming dose (10^9 vp), all mice exhibited protection against B16-OVA melanoma following treatment with Ad5.SIINFEKL (10^9 vp), with or without RMD+IBET151 (Fig. S1E-G).

Increased protein vaccine-elicited cellular immune response following RMD+IBET151 treatment provides CD8 T cell-mediated melanoma protection.

To determine whether the doubling in frequency and number of antigen-specific CD8 T cells following the combined administration of RMD+IBET151 was applicable to a range of vaccination platforms and regimens, we tested its effect on a protein-adjuvant based immunization regimen. Following the subcutaneous immunization of mice with OVA protein adjuvanted with CpG in an accelerated prime-boost-boost regimen, mice that received RMD +IBET151 at boost exhibited a significantly greater (> two-fold; $^{**}p < 0.01$ after 1st boost; $^{***}p < 0.001$ after 2nd boost) frequency of circulating SIINFEKL+CD8 T cells in the blood (Fig. 2A). This effect was also observed with OVA protein adjuvanted with the STING agonist CDN (Fig. S2A). To evaluate the efficacy of RMD+IBET151 treatment upon vaccination against melanoma tumor establishment, mice were primed subcutaneously with OVA+CpG, boosted days 14 and 28 with OVA+CpG ± RMD+IBET151, followed by the subcutaneous injection of 500,000 B16-OVA cells at day 48 (Fig. 2B; SIINFEKL+CD8 T cell frequency, Fig. S2B). The treatment of mice with RMD+IBET151 or PBS/DMSO alone, without vaccination, had no effect on tumor establishment, with all mice bearing tumors by day 8 and all mice sacrificed by day 24 (after tumor injection) due to tumor area exceeding 100 mm^2 (Fig. 2C). Only 50% of OVA+CpG vaccinated mice established melanoma and were subsequently sacrificed, with the tumors appearing between days 15 and 38 after their injection (Fig. 2C). Strikingly, vaccination with OVA+CpG in combination with RMD +IBET151 treatment resulted in complete prevention of melanoma establishment for the length of the study (90 days). 0 out of 8 of the OVA+CpG + RMD+IBET151 treated mice presented any measurable tumor load, resulting in a significant survival benefit over OVA +CpG vaccination alone (*, $p = 0.025$; Fig. 2C).

We examined the involvement of CD8 T cells in the antitumor effects observed following the OVA+CpG + RMD+IBET151 combination therapy. After the vaccination regimen, and one day prior to injection of 500,000 B16-OVA tumor cells, CD8 T cells were depleted *in vivo* using a specific mAb against murine CD8a. This CD8 T cell depletion was maintained weekly. All CD8 T cell depleted mice developed tumors and all were sacrificed by day 40 due to excessive tumor size ($^{***}p = 0.0001$), revealing a major role for CD8 T cells in the tumor protection conferred following OVA+CpG + RMD+IBET151 combination therapy (Fig. 2D).

Increased vaccine-elicited CD8 T cell responses following RMD+IBET151 treatment confer superior Listeria monocytogenes protection.

Having observed an effect of RMD+IBET151 treatment on anti-tumor immunity, we wanted to determine the effect on anti-pathogen immunity. As such, we assessed the protective role of RMD+IBET151 treatment on vaccination against *Listeria monocytogenes*, a bacterial model for CD8 T cell meditated protection. Mice were vaccinated with Ad26.OVA – Ad5.SIINFEKL, with or without RMD+IBET151 treatment at boost (Fig. 3A), and challenged intravenously with 5×10^5 colony forming units (CFU) of recombinant *Listeria monocytogenes* expressing OVA. RMD+IBET151 treatment during boosting vaccination afforded a significant reduction in *L. monocytogenes* load in the spleen of challenged mice ($^{***}p < 0.001$; Fig. 3B). In addition to boosting the response to adenoviral vaccination, mice that received RMD+IBET151 during protein (OVA+CpG) vaccination exhibited a significant reduction in *L. monocytogenes* bacterial load in the spleen at day two following infection ($^{*}p < 0.05$; Fig. 3C).

RMD+IBET151 treatment alters limited genes in adenoviral and protein vaccine elicited CD8 T cells.

Given the multifaceted involvement of epigenetic control, and thus the broad transcriptional impact that inhibition of HDAC and BET could result in, we sought to understand the transcriptional state of the vaccine elicited CD8 T cells following RMD+IBET151 treatment. To examine this, mice were vaccinated by either the Ad26-Ad5 prime-boost (Fig. 4A), or the OVA+CpG prime-boost-boost (Fig. 4C), regimen with either RMD+IBET151 or PBS/DMSO treatment during boost. Seven days after final vaccine boost, SIINFEKL+ CD8 T cells from the spleen of vaccinated mice were sorted, and their transcriptome profiling performed by RNA-Seq. Multidimensional analysis of the full transcriptomic profile of RMD+IBET151 treated and untreated groups revealed a high level of similarity between the two (Fig. 4B+D), indicating RMD+IBET151 treatment is not affecting the global gene expression profile of CD8 T cell. Whilst the global pattern was similar there were differences observed in the expression of pro- and anti-apoptotic genes. The addition of RMD+IBET151 to either protein or adenoviral vaccination regimens led to a down-regulation of the pro-apoptotic genes *Tnfrsf21* (Adenovirus: FC= −7.422; Protein: FC= −0.865), *Casp9* (Adenovirus: FC= −0.974; Protein: FC= −1.052) and *Tnfrsf25* (Adenovirus: FC= −0.851; Protein: FC= −0.771), and the up-regulation of the anti-apoptotic genes *Igf1r* (Adenovirus: FC= 1.205; Protein: FC= 1.251) and *Bcl2* (Adenovirus: FC= 0.519; Protein: FC= 0.724) relative to untreated controls (Fig. 4E).

Likewise, there was differential expression of genes related to chromatin modification and the enrichment of HDAC related pathways (Fig 4F), consistent with the fact that RMD and IBET151 are HDAC and BET domain inhibitors respectively.

RMD+IBET151 treatment increases IL-6 production and enhances CD8 T cell proliferation.

Pathways enrichment analysis revealed the differential expression of genes in the IL6/JAK/STAT3 pathway following RMD+IBET151 treatment (Fig. 5A), and this was consistent for both adenoviral and protein vaccination (Fig. 5B). In addition, Luminex analysis on serum samples from 6 h after Ad5.Gag vaccination revealed a significant increase in IL-6 concentration in RMD+IBET151 treated mice over PBS/DMSO control treated mice (***$p < 0.001$) (Fig. 5C). Subsequent daily high-dose administration of rIL-6 was capable of augmenting CD8 T cell numbers to that of RMD+IBET151 treatment alone during Ad26-Ad5 vaccination (Fig. 5D). Together these data indicate a role for IL-6 and its subsequent intracellular signaling cascade in enhancing CD8 T cell proliferation following treatment with RMD+IBET151.

RMD+IBET151 administration augments vaccine elicited antibody responses and confers superior protection against Influenza infection.

Having characterized the vaccine-elicited cellular immune responses following RMD+IBET151 we sought to investigate any effect by the treatment upon vaccine elicited humoral immune responses. Mice were vaccinated i.m. with Ad5.SIV Env (10^9 vp) and Ad26.SIV Env (10^9 vp) in heterologous prime-boost regimen, with or without RMD+IBET151 treatment at boost. 14 days after final boost, mice were bled, and serum IgG specific to the vaccine antigen SIV Env was quantified by quantitative ELISA. For both Ad26-Ad5 and Ad5-Ad26 regimens, the treatment with RMD+IBET151 significantly (*$p < 0.05$) increased the specific serum IgG concentrations elicited (Fig. S3A). The dual combination of RMD+IBET151 elicited greater serum IgG concentrations than either RMD or IBET151 treatment alone (Fig. S3A). To assess whether this was applicable to protein and adjuvant vaccination as well, mice were vaccinated s.c. with OVA+CpG in a prime-boost-boost regimen, with or without RMD+IBET151 treatments at boost. As with adenoviral vaccination, the treatment with RMD+IBET151 significantly (*$p < 0.05$) increased the OVA-specific serum IgG concentrations elicited, from a mean of 404 ng/ml to 816 ng/ml (Fig. S3B). Further characterization of the elicited IgG response revealed a significant shift in the IgG isotype following RMD+IBET151 treatment. With both adenoviral (Fig. S3C) and protein in adjuvant (Fig. S3D) vaccination, RMD+IBET151 treatment preferentially increased the induction of IgG1, while not affecting the induction of IgG2a. Mice vaccinated with HA protein in combination with RMD+IBET151 conferred greater protection against H1N1 Influenza (strain A/California/7/2009) infection, as observed by a reduction in weight loss, compared to HA vaccination alone (Day 5, *** $p < 0.001$; Day 6 and 7, **** $p < 0.0001$) (Fig. S3E). This correlated with an increase in both the serum HA-specific IgG concentration (Fig. S3F) and HA-specific CD8 T cell frequency in mice that received RMD+IBET151 (Fig. S3G).

Discussion

In this study, we demonstrate that the combined inhibition of the epigenetic regulators HDAC and BET augment vaccine-elicited cellular and humoral immune responses. This effect translates across different vaccine platforms, and confers superior anti-tumor efficacy against melanoma both therapeutically and prophylactically. We show that CD8 T cells mediate this anti-tumor efficacy, and RMD+IBET151 treatment enhances protection against the bacteria *Listeria monocytogenes,* and against the virus Influenza H1N1.. RNA-Seq analysis of CD8 T cells reveal only limited transcriptional differences following RMD +IBET151 treatment. These include apoptotic and IL-6/JAK/STAT3 related genes, concordant with IL-6 being preferentially expressed following RMD+IBET151 administration. The exogenous administration of IL-6 following vaccination recapitulates the increase in antigen-specific CD8 T cell number to that of RMD+IBET151 treatment.

The control of cellular immune responses, including the differentiation of naïve T cells into memory or effector cells, is choreographed by the epigenetic regulation of transcription factors (28). It has been demonstrated that epigenetic modifications, in particular histone modifications and DNA methylation, controls the transcription of effector molecules (e.g. IFN-γ, IL-2, granzyme b and perforin) through restricting chromatin access to transcription factors and polymerase (29–31). We observed no adverse effects on the vaccine elicited CD8 T cells following the inhibition of HDAC and BET during vaccination, with their cell-killing ability maintained and their transcriptional profiles near-identical. This may be due to the epigenetic inhibition being provided alongside multiple signals from vaccination, or due to the specific nature of the epigenetic inhibitor drugs RMD and IBET151. Previous research has revealed that HDAC and BET inhibitors induce similar genes, corroborating our observations of only few differentially expressed genes following RMD+IBET151 treatment (2).

We report that the combination of RMD+IBET151 during vaccination increases the production of IL-6, as measured in the serum by Luminex. Furthermore, we observe a greater gene expression signature for IL-6/JAK/STAT3 signaling in CD8 T cells following vaccination with RMD+IBET151. However, previous use of IBET151 has shown it to selectively block the production of IL-6 (32). Though not *in vivo* and not in combination with HDAC inhibition or vaccine stimulation, the previous study revealed that IBET151 interacts with the binding of BRD4 to the IL-6 promoter. Therefore there is a known molecular interaction between IBET151 and the IL-6 promoter, as well as with the BRD controlled promoters of TNF and IL-1b (33), for which we also saw increased production following RMD+IBET151 treatment. Future work will be needed to tease out the role of IL-6 and other pathways after RMD+IBET151 treatment. This may include depletion or supplementation of IL-6 prior to melanoma, Listeria or Influenza challenges to fully assess the cytokine’s involvement in their protection.

IL-6 has been previously shown to have pleiotropic activity on the differentiation and function of T cells. IL-6 promotes the specific differentiation of naïve CD4 T cells, performing a key function in linking the innate and acquire immune response (34), and is indispensable for Th17 differentiation (35). Relevant to the findings of this study, Okada *et*

al. previously revealed that IL-6 induced the differentiation of CD8 T cells into cytotoxic T cells (36). It has been further revealed that IL-6 also promotes T-follicular helper-cell differentiation which regulates immunoglobulin synthesis and IgG4 production in particular (37), and can induce the differentiation of activated B cells into antibody-producing plasma cells.

Combined HDAC and BET inhibitor therapy has also shown superiority over monotherapy for testicular germ cell cancer (4) and melanoma (3). However these observations were in nude mice lacking an adaptive immune system. This indicates that alternate modes of action of combined HDAC and BET inhibition, independent of immunological mechanisms, are also at play. These may include anti-angiogenesis or the activation of pro-apoptotic pathways in the tumor cells themselves (3). We see indication of this with therapeutic RMD +IBET151 treatment (without vaccination) slightly reducing melanoma growth compared to vehicle alone. However, in all cases, the combined administration of RMD+IBET151 with vaccination greatly improved melanoma protection over RMD+IBET151 treatment alone.

Following our observations that the HDAC and BET inhibitor need to be administered in combination, future experiments should build upon this. One could utilize the recently synthesized dual HDAC/BET small molecule inhibitor DUAL946 (38). The dual inhibition of BET and HDAC proteins has been confirmed *in vitro* and has shown cellular activity in cancer cells, suggesting that our observation maybe recapitulated with this single inhibitor in concert with vaccination.

The effect of epigenetic inhibition on vaccination warrants further investigation. We believe this study to be the first assessment of epigenetic inhibition on the immunogenicity of viral-vectored and protein-based vaccines, with HDAC inhibition previously investigated with autologous tumor cell-based vaccines. Such HDAC inhibition was shown to enhance MHC class II, CD40 and B7–1/2 expression on B16 cell-based vaccines, and correspondingly promoted the immune killing of autologous B16 melanoma cells via CD8 T cell induction (39–41). Our data indicates that this epigenetic enhancement expands beyond cellular vaccines to both protein and viral-vectored based vaccines, allowing greater translational use of the strategy.

This is the first time that these epigenetic modulators have been shown to increase vaccine efficacy via augmentation of antigen-specific CD8 T cell responses. These data suggest a greater role for CD8 T cell responses for melanoma than previously appreciated, and opens up new avenues to increasing vaccine elicited immune responses for improving cancer vaccine efficacy.

Supplementary Material

Refer to Web version on PubMed Central for supplementary material.

Acknowledgments

We thank the CVVR Flow Cytometry core for assistance with cell sorting, the NIH Tetramer Core Facility (Emory University) for provision of MHC class I monomers, and the Dana-Farber Cancer Institute for RNA-Seq.

ABZ, KDM, DJI and DHB conceived and designed the study. ABZ, KDM and NMP performed and analyzed the experiments. RAL, PPM, ENB, EK and JST helped with experiments. MA analyzed the RNA-Seq experiment. ABZ and RAL prepared the figures. ABZ and DHB wrote the paper.

Acknowledgments

Grant Support

DJI is an investigator of the Howard Hughes Medical Institute. PPM was supported by NIH (1K22 AI118421), ACS (IRG-15–173-21), and CFAR (P30 AI117943) grants. DHB was supported by NIH (AI096040, AI124377, AI126603, AI128751, AI129797, OD024917) and Ragon Institute grants.

References

1. Mazur PK, Herner A, Mello SS, Wirth M, Hausmann S, Sanchez-Rivera FJ, Lofgren SM, Kuschma T, Hahn SA, Vangala D, Trajkovic-Arsic M, Gupta A, Heid I, Noel PB, Braren R, Erkan M, Kleeff J, Sipos B, Sayles LC, Heikenwalder M, Hessmann E, Ellenrieder V, Esposito I, Jacks T, Bradner JE, Khatri P, Sweet-Cordero EA, Attardi LD, Schmid RM, Schneider G, Sage J, and Siveke JT. 2015 Combined inhibition of BET family proteins and histone deacetylases as a potential epigenetics-based therapy for pancreatic ductal adenocarcinoma. Nat Med 21: 1163–1171. [PubMed: 26390243]
2. Bhadury J, Nilsson LM, Muralidharan SV, Green LC, Li Z, Gesner EM, Hansen HC, Keller UB, McLure KG, and Nilsson JA. 2014 BET and HDAC inhibitors induce similar genes and biological effects and synergize to kill in Myc-induced murine lymphoma. Proc Natl Acad Sci U S A 111: E2721-2730. [PubMed: 24979794]
3. Heinemann A, Cullinane C, De Paoli-Iseppi R, Wilmott JS, Gunatilake D, Madore J, Strbenac D, Yang JY, Gowrishankar K, Tiffen JC, Prinjha RK, Smithers N, McArthur GA, Hersey P, and Gallagher SJ. 2015 Combining BET and HDAC inhibitors synergistically induces apoptosis of melanoma and suppresses AKT and YAP signaling. Oncotarget 6: 21507–21521. [PubMed: 26087189]
4. Jostes S, Nettersheim D, Fellermeyer M, Schneider S, Hafezi F, Honecker F, Schumacher V, Geyer M, Kristiansen G, and Schorle H. 2017 The bromodomain inhibitor JQ1 triggers growth arrest and apoptosis in testicular germ cell tumours in vitro and in vivo. J Cell Mol Med 21: 1300–1314. [PubMed: 28026145]
5. Bethune MT, and Joglekar AV. 2017 Personalized T cell-mediated cancer immunotherapy: progress and challenges. Curr Opin Biotechnol 48: 142–152. [PubMed: 28494274]
6. Couzin-Frankel J 2013 Breakthrough of the year 2013. Cancer immunotherapy. Science 342: 1432–1433. [PubMed: 24357284]
7. Zhang JA, Mortazavi A, Williams BA, Wold BJ, and Rothenberg EV. 2012 Dynamic transformations of genome-wide epigenetic marking and transcriptional control establish T cell identity. Cell 149: 467–482. [PubMed: 22500808]
8. Scharer CD, Barwick BG, Youngblood BA, Ahmed R, and Boss JM. 2013 Global DNA methylation remodeling accompanies CD8 T cell effector function. J Immunol 191: 3419–3429. [PubMed: 23956425]
9. Russ BE, Olshanksy M, Smallwood HS, Li J, Denton AE, Prier JE, Stock AT, Croom HA, Cullen JG, Nguyen ML, Rowe S, Olson MR, Finkelstein DB, Kelso A, Thomas PG, Speed TP, Rao S, and Turner SJ. 2014 Distinct epigenetic signatures delineate transcriptional programs during virus-specific CD8(+) T cell differentiation. Immunity 41: 853–865. [PubMed: 25517617]
10. Kaufman DR, De Calisto J, Simmons NL, Cruz AN, Villablanca EJ, Mora JR, and Barouch DH. 2011 Vitamin A deficiency impairs vaccine-elicited gastrointestinal immunity. J Immunol 187: 1877–1883. [PubMed: 21765014]
11. Roberts DM, Nanda A, Havenga MJ, Abbink P, Lynch DM, Ewald BA, Liu J, Thorner AR, Swanson PE, Gorgone DA, Lifton MA, Lemckert AA, Holterman L, Chen B, Dilraj A, Carville A, Mansfield KG, Goudsmit J, and Barouch DH. 2006 Hexon-chimaeric adenovirus serotype 5 vectors circumvent pre-existing anti-vector immunity. Nature 441: 239–243. [PubMed: 16625206]

12. Shen H, Slifka MK, Matloubian M, Jensen ER, Ahmed R, and Miller JF. 1995 Recombinant Listeria monocytogenes as a live vaccine vehicle for the induction of protective anti-viral cell-mediated immunity. Proc Natl Acad Sci U S A 92: 3987–3991. [PubMed: 7732018]
13. Bishton MJ, Gardiner EE, Harrison SJ, Prince HM, and Johnstone RW. 2013 Histone deacetylase inhibitors reduce glycoprotein VI expression and platelet responses to collagen related peptide. Thromb Res 131: 514–520. [PubMed: 23642854]
14. Wilson AJ, Lalani AS, Wass E, Saskowski J, and Khabele D. 2012 Romidepsin (FK228) combined with cisplatin stimulates DNA damage-induced cell death in ovarian cancer. Gynecol Oncol 127: 579–586. [PubMed: 23010348]
15. Dawson MA, Prinjha RK, Dittmann A, Giotopoulos G, Bantscheff M, Chan WI, Robson SC, Chung CW, Hopf C, Savitski MM, Huthmacher C, Gudgin E, Lugo D, Beinke S, Chapman TD, Roberts EJ, Soden PE, Auger KR, Mirguet O, Doehner K, Delwel R, Burnett AK, Jeffrey P, Drewes G, Lee K, Huntly BJ, and Kouzarides T. 2011 Inhibition of BET recruitment to chromatin as an effective treatment for MLL-fusion leukaemia. Nature 478: 529–533. [PubMed: 21964340]
16. Barber DL, Wherry EJ, Masopust D, Zhu B, Allison JP, Sharpe AH, Freeman GJ, and Ahmed R. 2006 Restoring function in exhausted CD8 T cells during chronic viral infection. Nature 439: 682–687. [PubMed: 16382236]
17. Tsukamoto H, Senju S, Matsumura K, Swain SL, and Nishimura Y. 2015 IL-6-mediated environmental conditioning of defective Th1 differentiation dampens antitumour immune responses in old age. Nat Commun 6: 6702. [PubMed: 25850032]
18. Knudsen JG, Murholm M, Carey AL, Bienso RS, Basse AL, Allen TL, Hidalgo J, Kingwell BA, Febbraio MA, Hansen JB, and Pilegaard H. 2014 Role of IL-6 in exercise training- and cold-induced UCP1 expression in subcutaneous white adipose tissue. PLoS One 9: e84910. [PubMed: 24416310]
19. Provine NM, Larocca RA, Aid M, Penaloza-MacMaster P, Badamchi-Zadeh A, Borducchi EN, Yates KB, Abbink P, Kirilova M, Ng'ang'a D, Bramson J, Haining WN, and Barouch DH. 2016 Immediate Dysfunction of Vaccine-Elicited CD8+ T Cells Primed in the Absence of CD4+ T Cells. J Immunol 197: 1809–1822. [PubMed: 27448585]
20. Barouch DH, Pau MG, Custers JH, Koudstaal W, Kostense S, Havenga MJ, Truitt DM, Sumida SM, Kishko MG, Arthur JC, Korioth-Schmitz B, Newberg MH, Gorgone DA, Lifton MA, Panicali DL, Nabel GJ, Letvin NL, and Goudsmit J. 2004 Immunogenicity of recombinant adenovirus serotype 35 vaccine in the presence of pre-existing anti-Ad5 immunity. J Immunol 172: 6290–6297. [PubMed: 15128818]
21. Rotzschke O, Falk K, Stevanovic S, Jung G, Walden P, and Rammensee HG. 1991 Exact prediction of a natural T cell epitope. Eur J Immunol 21: 2891–2894. [PubMed: 1718764]
22. Dobin A, Davis CA, Schlesinger F, Drenkow J, Zaleski C, Jha S, Batut P, Chaisson M, and Gingeras TR. 2013 STAR: ultrafast universal RNA-seq aligner. Bioinformatics 29: 15–21. [PubMed: 23104886]
23. Bolger AM, Lohse M, and Usadel B. 2014 Trimmomatic: a flexible trimmer for Illumina sequence data. Bioinformatics 30: 2114–2120. [PubMed: 24695404]
24. Robinson MD, McCarthy DJ, and Smyth GK. 2010 edgeR: a Bioconductor package for differential expression analysis of digital gene expression data. Bioinformatics 26: 139–140. [PubMed: 19910308]
25. Subramanian A, Tamayo P, Mootha VK, Mukherjee S, Ebert BL, Gillette MA, Paulovich A, Pomeroy SL, Golub TR, Lander ES, and Mesirov JP. 2005 Gene set enrichment analysis: a knowledge-based approach for interpreting genome-wide expression profiles. Proc Natl Acad Sci U S A 102: 15545–15550. [PubMed: 16199517]
26. Badamchi-Zadeh A, McKay PF, Holland MJ, Paes W, Brzozowski A, Lacey C, Follmann F, Tregoning JS, and Shattock RJ. 2015 Intramuscular Immunisation with Chlamydial Proteins Induces Chlamydia trachomatis Specific Ocular Antibodies. PloS one 10: e0141209.
27. Tan WG, Jin HT, West EE, Penaloza-MacMaster P, Wieland A, Zilliox MJ, McElrath MJ, Barouch DH, and Ahmed R. 2013 Comparative analysis of simian immunodeficiency virus gag-specific effector and memory CD8+ T cells induced by different adenovirus vectors. J Virol 87: 1359–1372. [PubMed: 23175355]

28. Nguyen ML, Jones SA, Prier JE, and Russ BE. 2015 Transcriptional Enhancers in the Regulation of T Cell Differentiation. Front Immunol 6: 462. [PubMed: 26441967]
29. Northrop JK, Thomas RM, Wells AD, and Shen H. 2006 Epigenetic remodeling of the IL-2 and IFN-gamma loci in memory CD8 T cells is influenced by CD4 T cells. Journal of immunology 177: 1062–1069.
30. Kersh EN, Fitzpatrick DR, Murali-Krishna K, Shires J, Speck SH, Boss JM, and Ahmed R. 2006 Rapid demethylation of the IFN-gamma gene occurs in memory but not naive CD8 T cells. Journal of immunology 176: 4083–4093.
31. Araki Y, Fann M, Wersto R, and Weng NP. 2008 Histone acetylation facilitates rapid and robust memory CD8 T cell response through differential expression of effector molecules (eomesodermin and its targets: perforin and granzyme B). Journal of immunology 180: 8102–8108.
32. Barrett E, Brothers S, Wahlestedt C, and Beurel E. 2014 I-BET151 selectively regulates IL-6 production. Biochim Biophys Acta 1842: 1549–1555. [PubMed: 24859008]
33. Nicodeme E, Jeffrey KL, Schaefer U, Beinke S, Dewell S, Chung CW, Chandwani R, Marazzi I, Wilson P, Coste H, White J, Kirilovsky J, Rice CM, Lora JM, Prinjha RK, Lee K, and Tarakhovsky A. 2010 Suppression of inflammation by a synthetic histone mimic. Nature 468: 1119–1123. [PubMed: 21068722]
34. Tanaka T, Narazaki M, and Kishimoto T. 2014 IL-6 in inflammation, immunity, and disease. Cold Spring Harb Perspect Biol 6: a016295.
35. Korn T, Bettelli E, Oukka M, and Kuchroo VK. 2009 IL-17 and Th17 Cells. Annu Rev Immunol 27: 485–517. [PubMed: 19132915]
36. Okada M, Kitahara M, Kishimoto S, Matsuda T, Hirano T, and Kishimoto T. 1988 IL-6/BSF-2 functions as a killer helper factor in the in vitro induction of cytotoxic T cells. Journal of immunology 141: 1543–1549.
37. Ma CS, Deenick EK, Batten M, and Tangye SG. 2012 The origins, function, and regulation of T follicular helper cells. J Exp Med 209: 1241–1253. [PubMed: 22753927]
38. Atkinson SJ, Soden PE, Angell DC, Bantscheff M, Chung C.-w., Giblin KA, Smithers N, Furze RC, Gordon L, Drewes G, Rioja I, Witherington J, Parr NJ, and Prinjha RK. 2014 The structure based design of dual HDAC/BET inhibitors as novel epigenetic probes. MedChemComm 5: 342–351.
39. Murakami T, Sato A, Chun NA, Hara M, Naito Y, Kobayashi Y, Kano Y, Ohtsuki M, Furukawa Y, and Kobayashi E. 2008 Transcriptional modulation using HDACi depsipeptide promotes immune cell-mediated tumor destruction of murine B16 melanoma. J Invest Dermatol 128: 1506–1516. [PubMed: 18185535]
40. Khan AN, Magner WJ, and Tomasi TB. 2004 An epigenetically altered tumor cell vaccine. Cancer Immunol Immunother 53: 748–754. [PubMed: 14997346]
41. Khan AN, Magner WJ, and Tomasi TB. 2007 An epigenetic vaccine model active in the prevention and treatment of melanoma. J Transl Med 5: 64. [PubMed: 18070359]

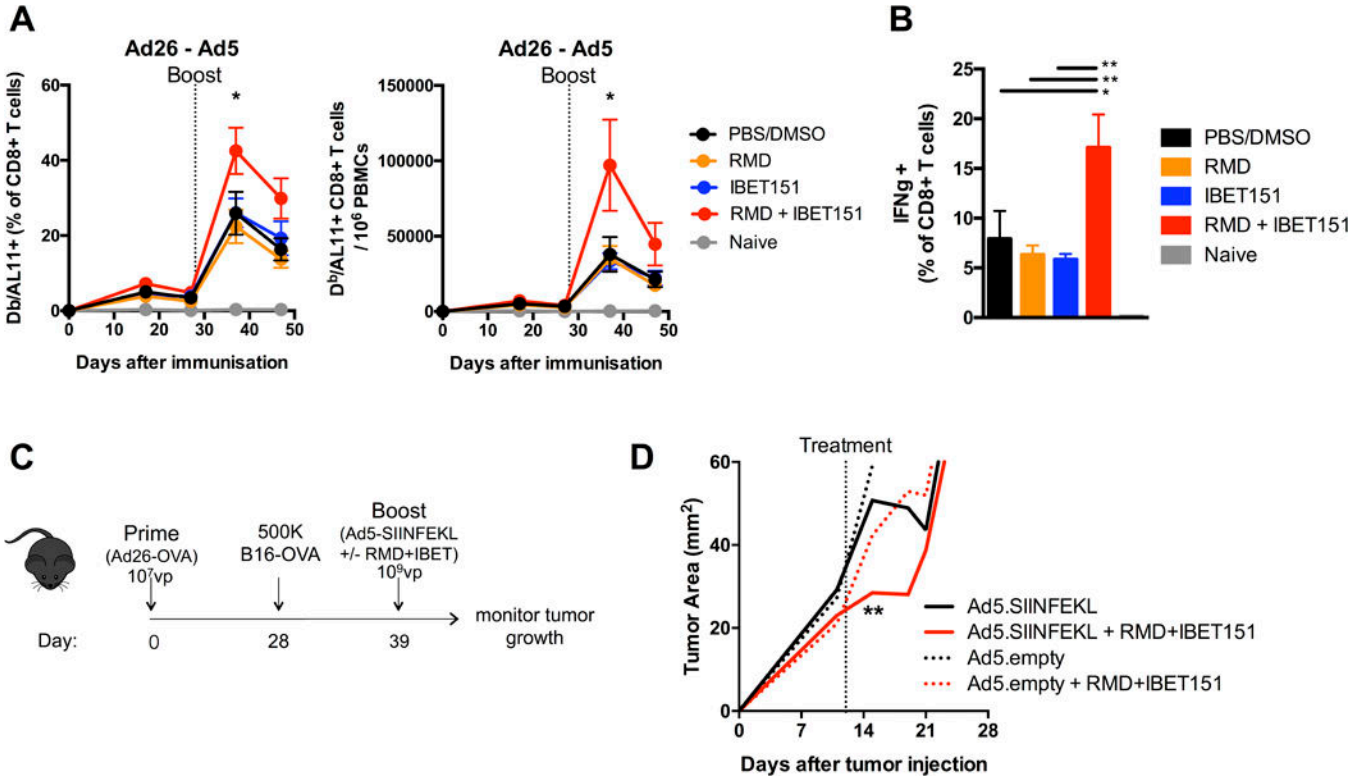

Fig. 1. RMD+IBET151 increases adenoviral-vector elicited T cell responses and confers superior protection against B16 melanoma.

(A-B) C57BL/6 mice were primed with Ad26 (10^9 vp) and boosted with Ad5 (10^9 vp) in combination with RMD, IBET151, RMD+IBET151 or PBS/DMSO. (A) Frequency and number of Gag-specific CD8 T cells in the blood. (B) Frequency of Gag-specific IFN-γ+ CD8 T cells in the spleen. (C) Experimental outline of B16-OVA challenge. (D) Tumor area measurements following B16-OVA tumor injection into primed mice and during therapeutic vaccination treatments. Each dot represents an individual mouse. $n = 4–10$ per group per experiment. Data are presented as means ± SEM. $^{*}p < 0.05$, $^{**}p < 0.01$, $^{***}p < 0.001$, Student T-test.

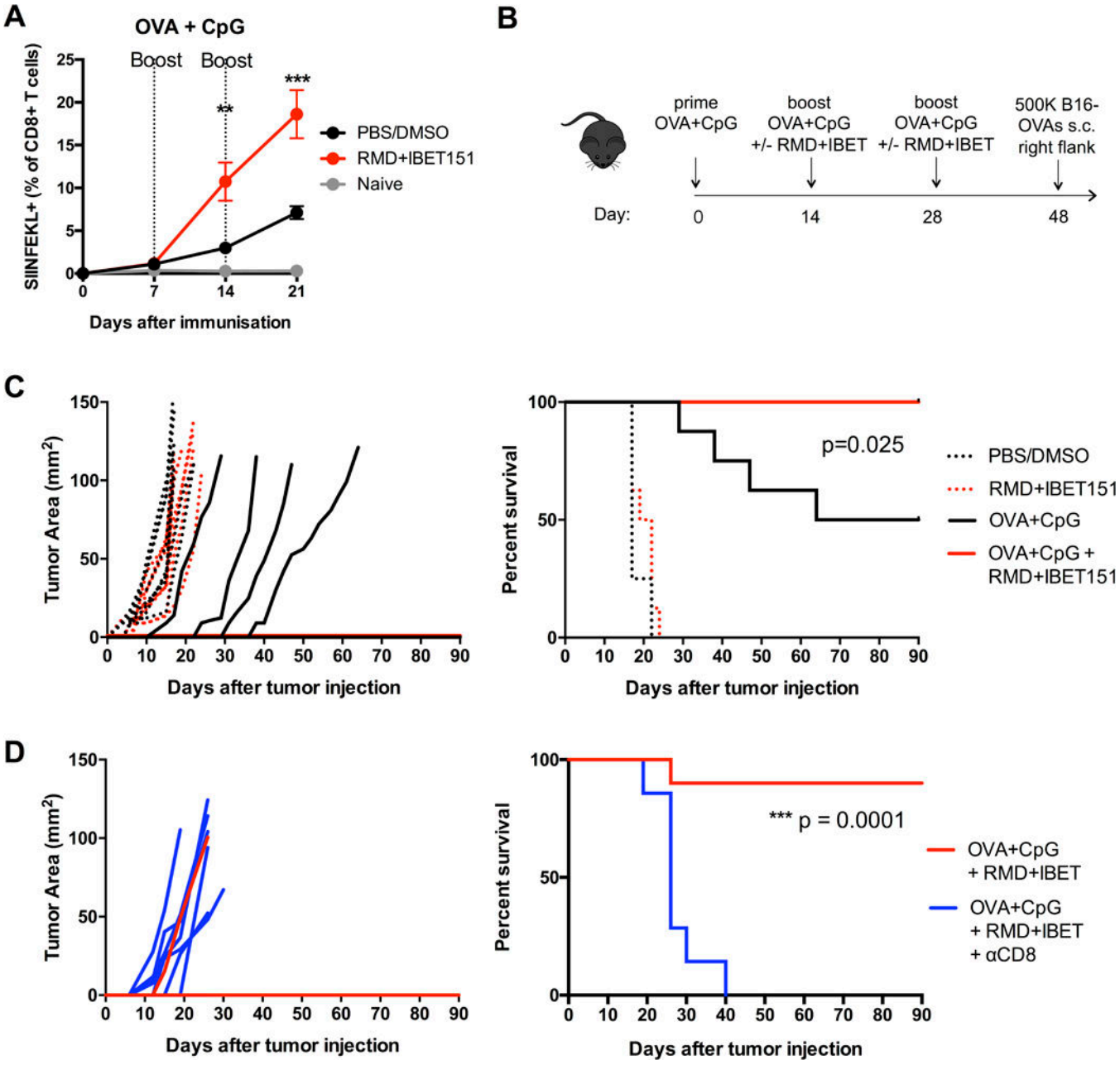

Fig. 2. RMD+IBET151 increases protein elicited T cell responses in an accelerated prime-boost regimen, conferring superior CD8 T cell-mediated melanoma protection.

(A-D) C57BL/6 mice were vaccinated subcutaneously with OVA protein adjuvanted with CpG, in combination with RMD+IBET151 or PBS/DMSO vehicle control. (A) Frequency of OVA-specific CD8 T cells in the blood. (B) Experimental outline of B16-OVA challenge. Tumor area measurements and survival curves following B16-OVA tumor injection into vaccinated mice (C), and CD8 T cell depleted vaccinated mice (D). Each dot represents an individual mouse. $n = 6–10$ per group per experiment. Data are presented as means ± SEM. $^{*}p < 0.05$, $^{**}p < 0.01$, $^{***}p < 0.001$, Student T-test. Survival significance by log-rank (Mantel-Cox) test.

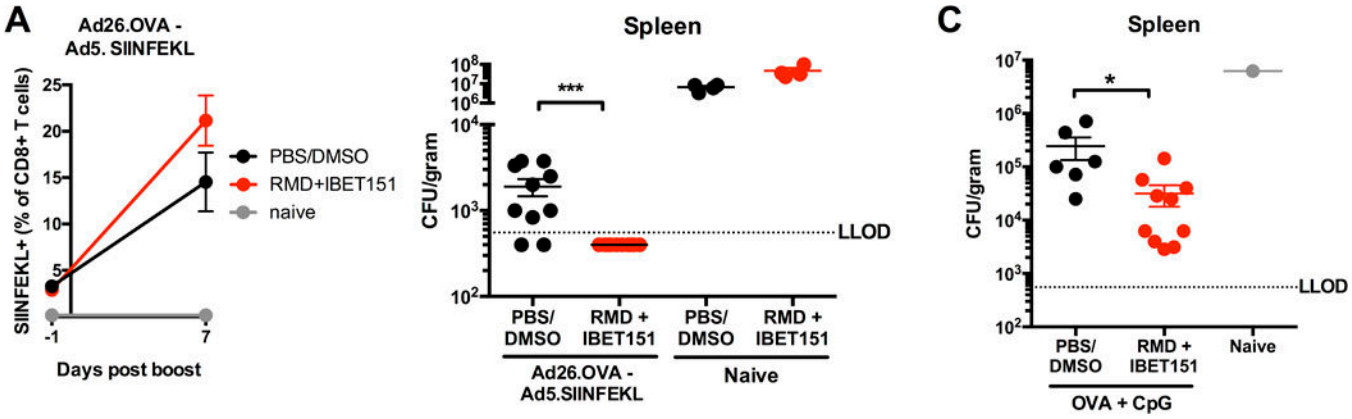

Fig. 3. RMD+IBET151 with vaccination provides enhanced protection against Listeria monocytogenes.

C57BL/6 mice were either (A) primed with Ad26 (10^9 vp) and boosted with Ad5 (10^9 vp), or (B) vaccinated subcutaneously with OVA protein adjuvanted with CpG, in combination with RMD, IBET151, RMD+IBET151 or PBS/DMSO. (A-B) *L. monocytogenes* titers in the spleen two days after challenge. Each dot represents an individual mouse. $n = 4–10$ per group per experiment. Data are presented as means ± SEM. $^{*}p < 0.05$, $^{**}p < 0.01$, $^{***}p < 0.001$, Student T-test.

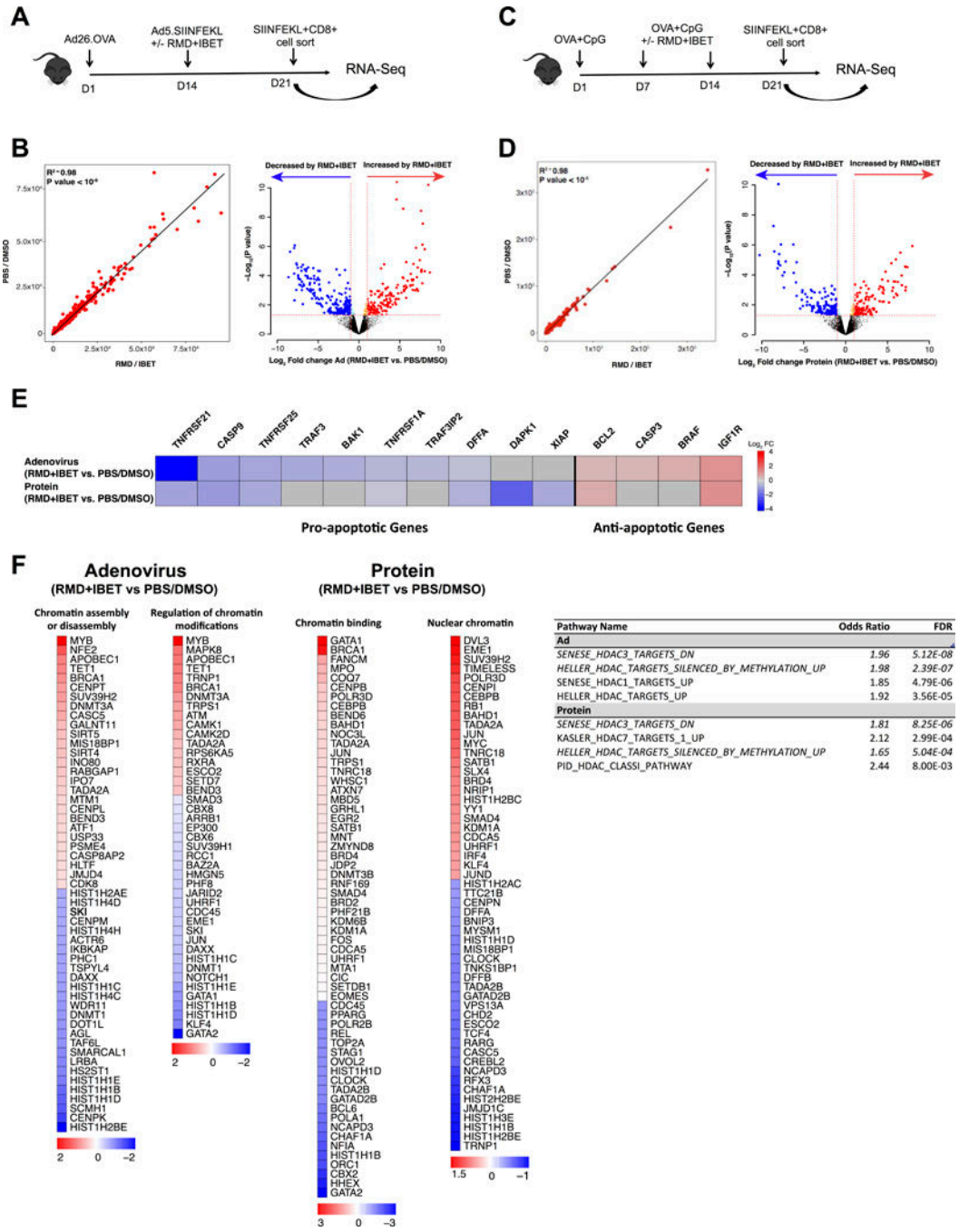

Pathway Name	Odds Ratio	FDR
Ad		
SENESE_HDAC3_TARGETS_DN	*1.96*	*5.12E-08*
HELLER_HDAC_TARGETS_SILENCED_BY_METHYLATION_UP	*1.98*	*2.39E-07*
SENESE_HDAC1_TARGETS_UP	1.85	4.79E-06
HELLER_HDAC_TARGETS_UP	1.92	3.56E-05
Protein		
SENESE_HDAC3_TARGETS_DN	*1.81*	*8.25E-06*
KASLER_HDAC7_TARGETS_1_UP	2.12	2.99E-04
HELLER_HDAC_TARGETS_SILENCED_BY_METHYLATION_UP	*1.65*	*5.04E-04*
PID_HDAC_CLASSI_PATHWAY	2.44	8.00E-03

Fig. 4. Differential expression of apoptosis and chromatin related genes in CD8 T cells following RMD+IBET151 treatment.

(A+C) Experimental outline prior to antigen-specific CD8 T cell sorting and RNA-Seq. (B +D) Correlation graph and volcano plot of differentially expressed genes between RMD +IBET151 treated and PBS/DMSO treated SIINFEKL+ CD8 T cells. (E) Differentially expressed genes related to apoptosis. (F) Differentially enriched pathways following RMD +IBET151 treatment on adenoviral and protein vaccination related to chromatin modification and binding. $n = 5$ per group, C57BL/6 mice.

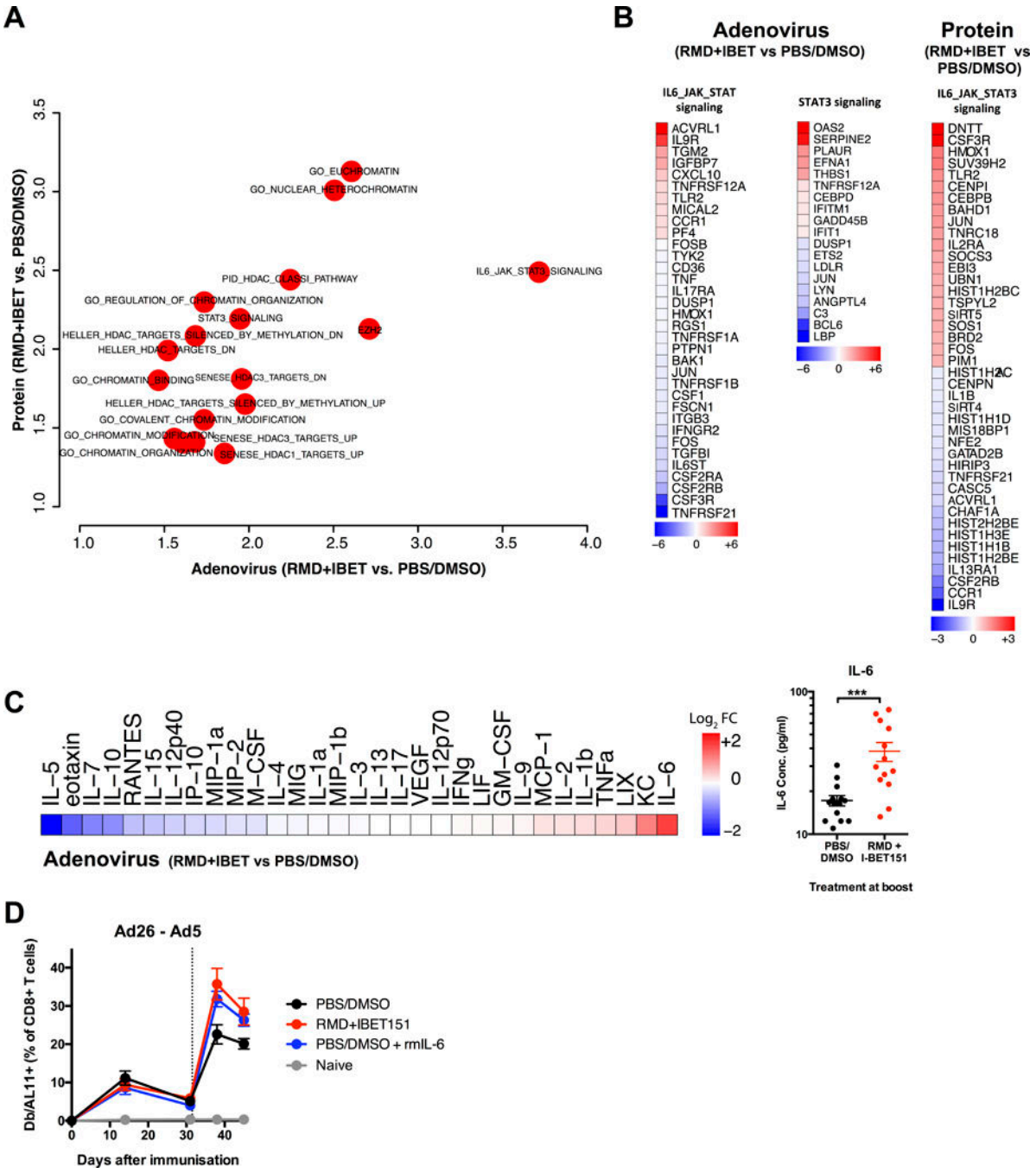

Fig. 5. Increased production of IL-6 and JAK/STAT3 signaling following RMD+IBET151 treatment at vaccination.

(A) Odds-ratio plot of pathways altered by RMD+IBET151 treatment on adenoviral and protein vaccination regimens. (B) Differentially expressed genes within IL6/JAK/STAT3 signaling following RMD+IBET151 treatment. (C) Heat map of cytokine/chemokine fold change (FC) of RMD+IBET151 treatment from PBS/DMSO treatment as measured by Luminex. Graph of individual mouse IL-6 serum concentrations (pg/ml) following either RMD+IBET151 treatment or PBS/DMSO treatment. Each dot represents an individual mouse. $n = 14$ per group. Data are presented as means ± SEM. $^{***}p < 0.001$, Student T-test.

(D) Frequency of Gag-specific CD8 T cells in the blood following Ad5.Gag (10^9 vp) boost in combination with RMD+IBET151, recombinant IL-6, or PBS/DMSO (n = 8–10 per group).